Acoustic beamforming through a thin plate using vibration measurements

Q. Leclere, Christophe Picard

Acoustic beamforming through a thin plate using vibration measurements.

ARTICLE *in* THE JOURNAL OF THE ACOUSTICAL SOCIETY OF AMERICA · JUNE 2015

Impact Factor: 1.56 · DOI: 10.1121/1.4921272 · Source: PubMed

2 AUTHORS:

Q. Leclère
Institut National des Sciences Appliquées d…
51 PUBLICATIONS **194** CITATIONS
SEE PROFILE

Christophe Picard
MicrodB
18 PUBLICATIONS **64** CITATIONS
SEE PROFILE

Acoustic beamforming through a thin plate using vibration measurements

Quentin Leclère[a)]
Laboratoire Vibrations Acoustique, INSA Lyon F-69621, France

Christophe Picard
MicrodB, Ecully 69130, France

(Dated: June 23, 2015)

The aim of this paper is to propose a methodology to localize acoustic sources from the measurement of airborne induced vibrations of a thin structure. Targeted applications are the identification of acoustic sources through a thin wall, with a potential filtration of the incident field, which may be of practical interest for instance when identifying exterior acoustic sources from the inside of a moving vehicle. Two methods are coupled here to achieve this purpose: the Force Analysis Technique (FAT), used to identify the parietal pressure field exciting the thin structure from vibration measurements, and beamforming, used for the localization of acoustic sources from the (FAT-)identified parietal pressure. The coupling of the two methods is studied first from a theoretical point of view, and an experimental proof of concept is then presented, showing the feasibility and relevance of the proposed approach.

PACS numbers: 4360Fg,4340Sk

I. INTRODUCTION

In many situations, one may be interested in the possibility of localizing acoustic sources from vibration measurements. This is typically the case if we want to localize an acoustic source through a wall: the vibration of the wall can be measured using an array of accelerometers, or using nearfield acoustic measurements on one side of the wall. The incident acoustic pressure field exciting the wall from the other side can then be identified, and used as an input for an acoustic source localization method. This is also the case if the structure is used as a filter: in cases when the incident acoustic pressure is disturbed by a turbulent boundary layer, the plate will act as a low-pass filter in the wavenumber domain, offering a tunable possibility of separating acoustic and aerodynamic fields. These situations are both encountered, for instance, in the issue of identifying exterior acoustic sources from the inside of a moving vehicle.

The aim of this paper is to propose a methodology coupling two methods to achieve this purpose. The first method, known as Force Analysis Technique (FAT)[1], utilizes measurements of plate displacement to estimate the load field which is exciting the plate. It has been first developed for beams and plates, and later has been extended to shells[2] and finite elements[3]. Some improvements have been proposed recently[4], extending the frequency range of application. The second method is beamforming, an acoustic source localization method based on acoustic array measurements. Initially developed for underwater acoustics[5], the method has been later extended to acoustics in air by Billingsley and Kinns's[6] (the acoustic telescope). In the proposed methodology, acoustic array measurements are replaced by the pressure field estimated using the FAT.

The idea to use vibration sensors through a thin structure for beamforming applications has been inspected in several papers for underwater ultrasound applications[7] or broadband sonar processing[8]. In these two papers, an analysis of the response of vibration based beamforming is provided in either space or wavenumber domains. More recently, vibration based beamforming has been studied to localize acoustic sources inside a cylindrical shell filled with heavy fluid[9]. The first contribution of the present work is the use of the FAT, usually implemented for the localization of structure borne sources, for the identification of an acoustic pressure field exciting a wall. Recent efforts in that domain might however be cited, concerning the identification of a diffuse field[10] or a turbulent boundary layer[11,12]. In these last works, the ability of the FAT to operate a filtering in the wavenumber domain has been observed experimentally. A second original aspect is to consider the issue of using FAT results for beamforming, from the theoretical point of view, considering the wavenumber behavior of both methods, and also pointing out some practical issues. This issue has, at the authors's knowledge, not yet been investigated in the literature.

The first part of the paper is dedicated to theoretical aspects. In sections II.A and II.B, basic principles of beamforming and FAT are recalled. Section II.C concerns the issue of coupling beamforming and FAT, considering their respective wavenumber domain responses, and the consequences on the useful frequency range. The second part of this work describes an experimental implementation of the proposed methodology, with a demon-

[a)]Electronic address: quentin.leclere@insa-lyon.fr

stration of the feasibility and reliability of the method.

II. THEORY

A. Acoustic beamforming

Acoustic beamforming is a source localization technique based on acoustic array measurements, introduced in the seventies by Billingley and Kins[6]. The idea is to delay and sum time signals from a set of microphones in order to estimate the arrival angle of farfield sources. Beamforming does not belong to the class of identification methods for acoustic source localization, like Nearfield Acoustic Holography[13], Equivalent source methods[14] or Inverse BEM[15]: with beamforming, the strength of each is identified independently from the others, while a global inversion (requiring regularization) is used by aforementioned approaches. It makes beamforming a remarkably robust approach, the limitations being a poor resolution in the low frequency range and a limited quantitative capability. Beamforming is choosen in this work for the sake of simplicity, it is however noteworthy that more sophisticated acoustic imaging techniques could also be coupled with the FAT.

In the frequency domain, the output of beamforming is the scalar product between the measured pressure and the pressure shape that would have been obtained if the waves were coming from angle θ. For a 1D uniformly spaced array of microphones, without any spatial weighting, the beamforming result is given by:

$$r(\omega,\theta) = \sum_{m=1}^{M} p(m,\omega) e^{-jm\Delta k_x}, \tag{1}$$

where $p(m,\omega)$ stands for the acoustic pressure measured at microphone m (Pa), Δ is the distance between two consecutive microphones , M is the total number of microphones, $k_x = k\sin(\theta)$ (rad/m), $k = \omega/c$ the acoustic wavenumber (rad/m), and c the sound speed (m/s).

The response of the antenna for the case of a plane wave of unitary amplitude and incidence Θ ($K_x = k\sin(\Theta)$) is thus given by:

$$r(\omega,\theta,\Theta) = \sum_{m=1}^{M} e^{jm\Delta(K_x - k_x)}. \tag{2}$$

This response has of course a maximum for $\theta = \Theta$, allowing the localization of the actual source position. A second maximum can occur for $|k_x - K_x| = 2\pi/\Delta$, if Shannon's criterion has not been met; this is called a grating lobe. This brings the maximum frequency limitation for an array of regular spatial sampling Δ:

$$\Delta < \frac{\lambda}{2}, \text{ or } \omega < \frac{\pi c}{\Delta}, \tag{3}$$

where $\lambda = c/f$ is the acoustic wavelength, f the frequency. The low frequency limit depends on the spatial dimensions of the array. Indeed, it can be stated that the low frequency limit is the minimum frequency above which the beamforming output has at least one totally destructive interference (null) within $\theta \in [-\pi/2, \pi/2]$, for $\Theta = 0$. These considerations bring out the low frequency limit of an array of length $N\Delta$:

$$\omega > \frac{2\pi c}{N\Delta}, \text{ or } f > \frac{c}{L}, \tag{4}$$

where $L = N\Delta$ is the array length.

B. Estimation of acoustic pressures from vibration measurements

The Force Analysis Technique[1,4] (FAT) is an experimental approach aiming at the inverse identification of the load field exciting a thin structure from vibration measurements. The basic principle is to directly solve the local equation of motion of a structure to identify locally the forcing term. For flexural beams and plates, this involves the estimation of fourth order spatial derivatives of the vibration field on a measurement mesh. For the flexural beam case, the actual (analytic) and identified forces per unit of length, noted p and $\tilde{p}$, respectively, are given by (cf. Refs.[1,16]):

$$p(x) = EI\frac{\partial^4 w}{\partial x^4}(x) - \rho S\omega^2 w(x), \tag{5}$$

$$\tilde{p}(x) = EI\mu^4\delta_\Delta^{4x}(x) - \rho S\omega^2 w(x), \tag{6}$$

where E, I, ρ, S are the physical parameters of the beam (Young's modulus, area moment of inertia, density and cross section area, respectively), $w(x)$ the transverse displacement of the beam, and with

$$\delta_\Delta^{4x}(x) = \frac{w_{-2} - 4w_{-1} + 6w_0 - 4w_{+1} + w_{+2}}{\Delta^4}, \tag{7}$$

where $w_{\pm l}(x) = w(x \pm l\Delta)$ is the measured displacement at 5 points surrounding the load identification point. Eq.(5) is simply the equation of motion of the flexural beam, establishing the local equilibrium between load, stiffness and inertia. In Eq. (6), $\delta_\Delta^{4x}(x)$ (developed in Eq. (7)) is a standard finite difference estimation of the fourth order spatial derivative of the displacement field $\frac{\partial^4 w}{\partial x^4}(x)$, on which rely the FAT. This estimation is obtained at the center of the finite difference scheme (point x) from the displacement at 5 points around this position on a measurement mesh with a regular spacing Δ. The finite difference scheme is then slided along the measurement mesh (point $x + \Delta$, $x + 2\Delta$ ...), so as to recover the load field with a spatial sampling Δ. μ^4 is an corrective factor, equal to unity when using the standard FAT[1], that has been introduced recently in a corrected version of the FAT[4] (called CFAT) to correct the bias effect caused by the finite difference approximation. This parameter is equal to:

$$\mu^4 = \frac{\Delta^4 k_N^4}{(2 - 2\cos(k_N\Delta))^2}, \tag{8}$$

where k_N is the natural wavenumber at the frequency ω (cf. Refs.[1,16]):

$$k_N^4 = \frac{\rho S}{EI}\omega^2. \tag{9}$$

The effect of the correction in CFAT has been studied in Ref.[4], its advantage is to improve the wavenumber domain response of the method when the discretization Δ used for the finite difference scheme is coarse, i.e. less than 4 points by structural wavelength. The effectiveness of the CFAT in the wavenumber domain is analyzed through the ratio between the actual pressure p and its CFAT estimate $\tilde{p}$:

$$E(\alpha) = \frac{\tilde{p}(\alpha)}{p(\alpha)} = \frac{\left(\frac{\sin(\alpha\pi/n)}{\sin(\pi/n)}\right)^4 - 1}{\alpha^4 - 1}, \tag{10}$$

where n corresponds to the number of measurement points by natural wavelength $n = 2\pi/(k_N\Delta)$ and $\alpha = k/k_N$ the normalized wavenumber. This wavenumber response, that can be interpreted as a spatial filter, is drawn in Fig. 1 for different values of n. As can be seen

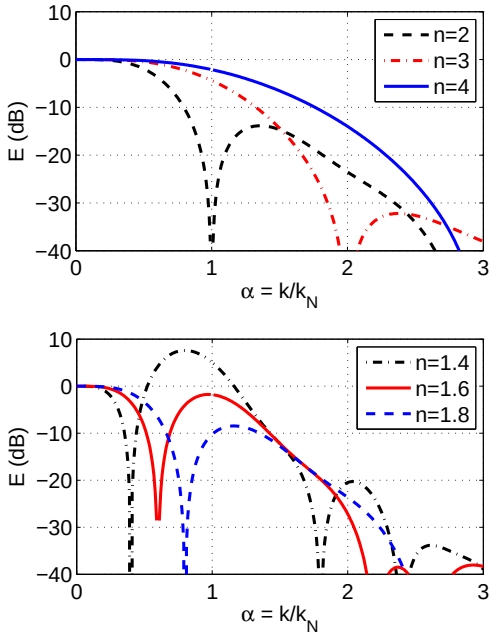

FIG. 1. (color online) Response of the CFAT filter in the wavenumber domain for different values of n (number of points by structural wavelength)

in Fig. 1, the response of CFAT is not perfect (i.e. equal to 0dB) in the whole wavenumber domain. The response to low wavenumbers is quite good, but the method is not able to recover correctly high wavenumbers, above a cutoff wavenumber increasing with n. For $n > 2$ (Fig. 1, top), high wavenumbers are simply attenuated. For lower values of n, the response is still quite flat for the low wavenumber domain, there is a first band-stop filter around the value $n - 1$, but secondary lobes in the high wavenumber domain becoming more and more energetic when n decreases. These secondary lobes have to be avoided, even if the excitation is known to be concentrated in the low wavenumber domain, because they will lead to an strong amplification of the measurement noise (that is spread over the whole wavenumber range). The limitation $n > 2$ (at least 2 points by flexural wavelength) leads to the following criterion:

$$\omega < \left(\frac{\pi}{\Delta}\right)^2 \sqrt{\frac{EI}{\rho S}}. \tag{11}$$

C. Simulation using CFAT results for beamforming

The CFAT, presented in the previous section, can be used to estimate the acoustic pressure exciting a thin structure from vibration measurements. This estimated pressure can then be used as input data for acoustic beamforming, notwithstanding the following points:

- for the one dimension case (the CFAT for flexural beams), the identified load is a force per unit length. This load can be converted into a pressure by dividing it by the beam's width, assuming that the acoustic pressure is constant along the beam's width (which is almost true if the beam's width is small as compared to the acoustic wavelength).

- The pressure identified by CFAT is not directly equal to the incident field, because of the diffraction effect of the structure used for vibration measurements. This important point is discussed in section II.E.

- the CFAT identifies without distinction the load on both sides of the considered structure (beam or plate). In order to assume that the identified load is equal to the parietal pressure on the source side only, the parietal pressure on the other side has to be significantly lower, which can be achieved if the structure is correctly baffled, and for frequencies where the transparency of the structure is low enough (this is generally not a limitation for the targeted frequency range of application).

The use of the CFAT for the identification of plane waves requires the consideration of its wavenumber response discussed in the previous section. The wavenumbers of any collection of farfield source signals will be concentrated between $k_x = 0$ (normal incidence) and $k_x = k$ (tangential incidence). Thus, the response of CFAT should be almost flat in this wavenumber range. For $n > 2$, the CFAT response will be considered as flat for $\alpha < n/3$ (cf. Fig. 1). The application of CFAT to plane waves thus brings:

$$\omega < \frac{2\pi c}{3\Delta}. \tag{12}$$

It can be noted that this criterion based on the CFAT lowpass filtering effect in the wavenumber domain is more demanding than the Shannon's criterion for acoustic beamforming (Eq. 3). This means that if CFAT

results are post processed as inputs for acoustic beamforming (which is the object of this work), a criterion a bit more severe than Shannon's has to be observed to avoid the CFAT bias effect. This is quite important to note, because beamforming is sometimes used above the Shannon's limit, that can be rightfully exceeded if it is a priori known that the angle of incidence of incoming plane waves is limited to a given angular range (no tangential waves).

To illustrate these considerations, the response of a microphone array based on the CFAT identification of the acoustic pressure is numerically studied. A linear array of 10 acoustic measurement points regularly spaced is considered. The structural CFAT criterion (eq. 11) is fulfilled ($n = 2.5$ points by structural wavelength). The response of the antenna is given in Fig. 2 for $\omega = \frac{2\pi c}{3\Delta}$ (upper frequency for the acoustical CFAT criterion) and $\omega = \frac{\pi c}{\Delta}$ (Shannon's limit for beamforming). Note that the estimation of the pressure by CFAT at extreme positions of the antenna requires 2 additional vibration measurement points on both sides, because of the finite difference scheme used for the estimation of the fourth order derivative (see eq. 7). The results obtained for conventional beamforming and CFAT-based beamforming are very similar for the first frequency ($\omega = \frac{2\pi c}{3\Delta}$, satisfying 3 points by acoustic wavelength). The main lobe is centered on the actual angle of incidence, its width broadening when the angle of incidence θ exceeds $\pi/4$. CFAT-based results are however slightly underestimated for incoming waves with an incidence angle around $\pi/2$ (near-tangential waves), because of the low response of the CFAT-based beamformer at higher wavenumbers or larger incident angles. This effect is much more pronounced for the second studied frequency, corresponding to the Shannon's limit for the spatial sampling ($\omega = \frac{\pi c}{\Delta}$, 2 points by acoustic wavelength). A secondary lobe at $\phi = \theta \mp \pi/2$ (due to aliasing) is observed for values of θ around $\pm\pi/2$ for conventional beamforming. This grating lobe is not observed on the CFAT-based beamforming, because of the CFAT filtering effect, that also filters out the main lobe for values of θ close to $\pi/2$.

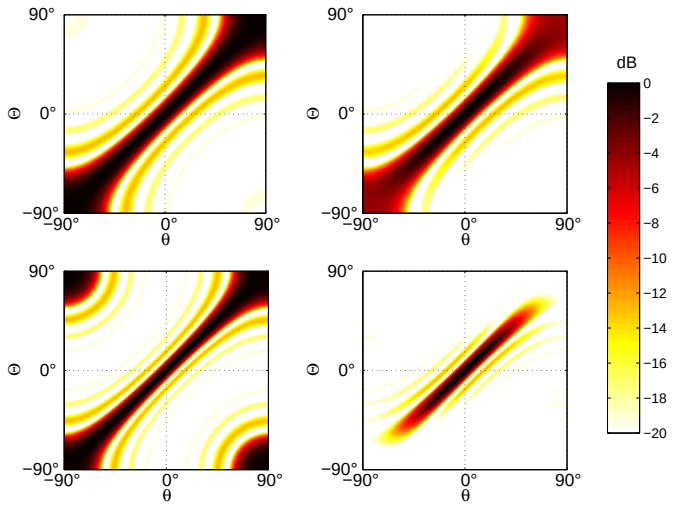

FIG. 2. (color online) Left: conventional beamforming response (function of θ) as a function of the actual incidence Θ. Right: CFAT-based beamforming response. Top: $\omega = \frac{2\pi c}{3\Delta}$ (3 points by acoustic wavelength). Bottom : $\omega = \frac{\pi c}{\Delta}$ (2 points by acoustic wavelength). dB scale, 20dB range.

D. Extension to two dimensions

The basic principles of beamforming and CFAT, and their interactions, have been presented in previous sections for the one dimensional case, for the sake of simplicity. However, the experimental implementation of the 1D case is not easy, because of the necessity to baffle the beam, in order to expose only one side of the structure to the acoustic load. Another point is that the beam's width has to be small as compared to the acoustic wavelength, which adds another frequency limitation to the method. These two problems are not encountered when dealing with the two dimensions version of CFAT-based beamforming. For the flexural plate case, the actual and identified forces per unit of area are given by (cf. Refs.[16],[18]):

$$\begin{aligned} p(x,y) &= D\nabla^4(w(x,y)) - \rho h\omega^2 w(x,y), && (13)\\ \tilde{p}(x,y) &= D\Phi_\Delta(x,y) - \rho h\omega^2 w(x,y), && (14)\\ \text{with}\quad \Phi_\Delta(x,y) &= \mu^4\delta_\Delta^{4x} + \mu^4\delta_\Delta^{4y} + 2\nu^4\delta_\Delta^{2x2y}, \end{aligned}$$

where $D = Eh^3/12/(1-\nu^2)$, h is the plate's thikness, ν the Poisson's ratio, ρ the density, δ_Δ^{4x}, δ_Δ^{4y}, and μ^4 are obtained as for the 1D case (Eq. 7 and 8), with k_N the natural wavelength of the plate:

$$k_N^4 = \frac{\rho h}{D}\omega^2. \qquad (15)$$

The term δ_Δ^{2x2y} is equal to:

$$\delta_\Delta^{2x2y} = \frac{1}{\Delta^4}\sum_{p=-1}^{1}\sum_{q=-1}^{1}\psi_{pq}w(x+p\Delta, y+q\Delta), \qquad (16)$$

$$\begin{aligned} &\text{with}\quad \psi_{00} = 4,\\ &\psi_{-10} = \psi_{10} = \psi_{0-1} = \psi_{01} = -2,\\ &\psi_{-1-1} = \psi_{11} = \psi_{1-1} = \psi_{-11} = 1, \end{aligned} \qquad (17)$$

and the correcting factor ν^4 is defined by:

$$\nu^4 = \frac{\Delta^4 k_N^4}{8\left[1-\cos(\frac{k_N\Delta}{\sqrt{2}})\right]^2} - \mu^4. \qquad (18)$$

It can be noted that if 5 points surrounding the load identification point are needed for the 1D case, the 2D case requires 13 points to assess the load at one point. When dealing with measurements on a regular grid, it means that the load will be assessable on the whole grid except a 2 point wide band at the edge.

The 2D implementation of CFAT has a low-pass filtering effect in the wavenumber domain, as is the case for the 1D implementation, see Ref.[4] for theoretical details. The

consequence on the identification of plane waves is similar in 2D as in 1D : incoming waves with high incidence angles will be underestimated if the number of points by acoustic wavelength is lower than 3 (cf. Eq. 12). The limitation concerning the sampling of the vibration field is the same as for the 1D case, i.e. 2 points by flexural wavelength. This brings the following HF limitation:

$$\omega < \left(\frac{\pi}{\Delta}\right)^2 \sqrt{\frac{D}{\rho h}}. \tag{19}$$

Concerning beamforming, the extension of the 1D formula (1) to 2D, for an angle of incidence θ over x and φ for y is simply:

$$s(\omega,\theta,\varphi) = \sum_{n=1}^{N}\sum_{m=1}^{M} p(n,m,\omega) e^{-jn\Delta k_x} e^{-jm\Delta k_y}, \tag{20}$$

where $p(n,m,\omega)$ stands for the acoustic pressure at point $(x,y) = (n\Delta, m\Delta)$, Δ is the distance between two consecutive microphones, $N \times M$ is the total number of microphones, $k_x = k\sin(\theta)\cos(\varphi)$ and $k_y = k\sin(\varphi)$ (rad/m).

E. Intrusivity of the measurement device

The acoustic pressure that is identified by CFAT is the parietal pressure on the instrumented structure (beam or plate). Of course, this pressure is not equal to the acoustic pressure at the same positions without the structure, because of diffraction effects. In other words, the CFAT-based beamforming is an intrusive approach, contrary to standard microphone array beamforming, whose intrusivity is generally negligible. This intrusivity can be partly corrected by an experimental or numerical study of the diffraction effects, that can then be taken into account in Eq. (1) or (20). Another possibility is simply to consider that the measured structure is inserted in an infinite rigid baffle. In this case, assuming that the transmission loss of the instrumented structure is high enough, ensuring a quasi-total reflection of incident waves, the parietal pressure is almost equal to twice the incident pressure.

These corrections are however somewhat limited by the fact that the incident pressure can also be modified by the measurement device if the reflected waves are once again reflected by another rigid body that is not taken into account, or the source's body itself. However, these effects can be assumed to be negligible in many situations, if the surface of the structure is small as compared to the surface of all other reflective bodies, and when other reflective bodies are sufficiently far from the structure.

III. EXPERIMENTAL VALIDATION

An experimental validation has been carried out for the proposed approach. An acoustic source has been placed in a semi-anechoic room, with a reflective floor (see Fig. 3). One wall is also reflective, in which a $40 \times 60cm^2$ opening is made towards a second room. A 1mm thick aluminium plate is mounted to close this window. The source is a compression driver, fed with a white noise signal through a power amplifier. It is placed at 1.3m from the reflective wall, with a direction of incidence $\theta = -25°, \varphi = 15°$ from the normal of the plate at the center of the plate. The presence of the reflective ground generates an image source, with the same azimuth θ, but with an elevation φ equal to $-57°$, that takes into account the distance between the ground and the center of the plate. The velocity of the plate is measured by

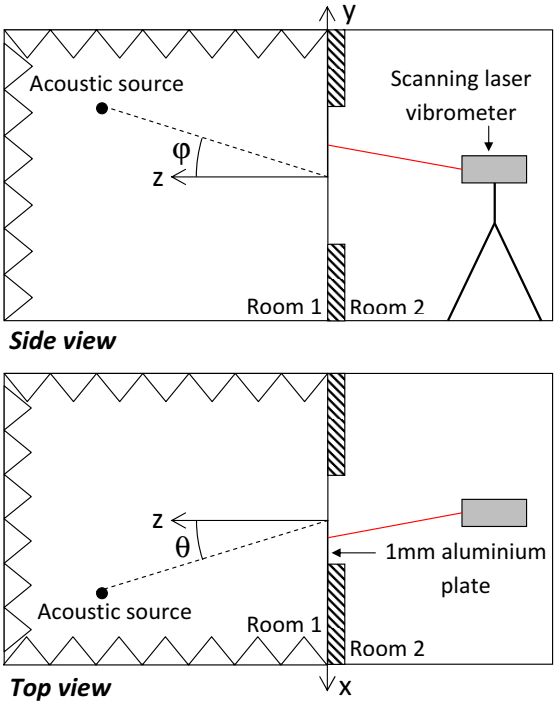

FIG. 3. (color online) Experimental setup. θ stands for the azimuth and ϕ for the elevation.

a scanning laser vibrometer placed in the second room. The scanning area is $31 \times 57cm^2$ with a regular grid of 25×37 points. The grid step Δ is equal to 16mm. The reference signal is a microphone placed in room 1, in the very nearfield of the plate. The transfer functions between the reference and the velocity is assessed at each point of the measurement grid, H1-estimator (ratio between the cross spectrum and reference autospectrum, cf. Eq. (21)), Hanning weighting, 20 averages. The velocity is then obtained by using the transfer function and the autospectrum of the reference averaged over all measurement points, as proposed in[17]:

$$V_i = H_{ir}^i \sqrt{\langle S_{rr} \rangle} = \frac{S_{ir}^i}{S_{rr}^i} \sqrt{\frac{1}{N}\sum_{j=1}^{N} S_{rr}^j} \tag{21}$$

where $H_{ir} = \frac{S_{ir}}{S_{rr}}$ is the H1 estimator of the transfer function between the velocity at point i and the pressure

measured at the reference microphone V_i/P_r, S^i_{ir} stands for the cross-spectrum between point i and reference r and S^j_{rr} for the reference autospectrum measured while the laser is pointing on position j.

Considering the frequency limitations established in the previous section, the maximum frequency related to the flexural wavelength (Eq. 19, 2 points by flexural wavelength) is equal to 9.5kHz, and the maximum frequency related to the CFAT-Beamforming coupling (Eq. 12, 3 points by acoustic wavelength) is equal to 7kHz.

In the first instance, the acoustic pressure is estimated using 2D CFAT (see section II.D). The identified pressure spectrum is compared to the reference (parietal microphone) for validation. The spectrum measured by the microphone and the pressure identified at the corresponding grid point are drawn in Fig. 4. The periodicity in the frequency domain of measured and identified pressure spectra is caused by the interferences between the direct path and the reflection by the ground. The two spectra are in very good concordance above 1.5kHz. below this frequency, the pressure identified by CFAT is largely overestimated. This is a well known problem of the method, for which a regularization filter is required for the low frequency range[1]. Several approaches can be implemented to improve FAT results in the low frequency domain, such as spatial filtering[18], or frequency-dependent adaptation of the finite difference scheme[19]. However, the frequency limit above which the method gives reasonable results without any regularization is about 1kHz in our case, it corresponds almost to the low frequency limit of beamforming obtained by Eq. (4). The method will thus be used without regularization in this work, for the sake of simplicity.

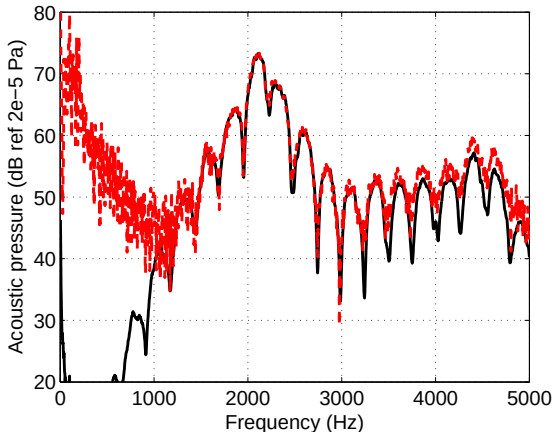

FIG. 4. (color online) Reference parietal microphone (solid), identified acoustic pressure at the corresponding grid point (dotted).

The 2D maps of the measured velocity and identified pressure are drawn in Fig. 5 at about 2.5 and 4kHz. The velocity maps are clearly dominated by components determined by the natural flexural wavelength of the plate. The pressure maps are dominated by wavenumbers resulting from the projection of the acoustic wavevector in the plate's plane. Interferences are clearly seen on these maps, corresponding to the interactions between the direct field and the field diffracted by the ground.

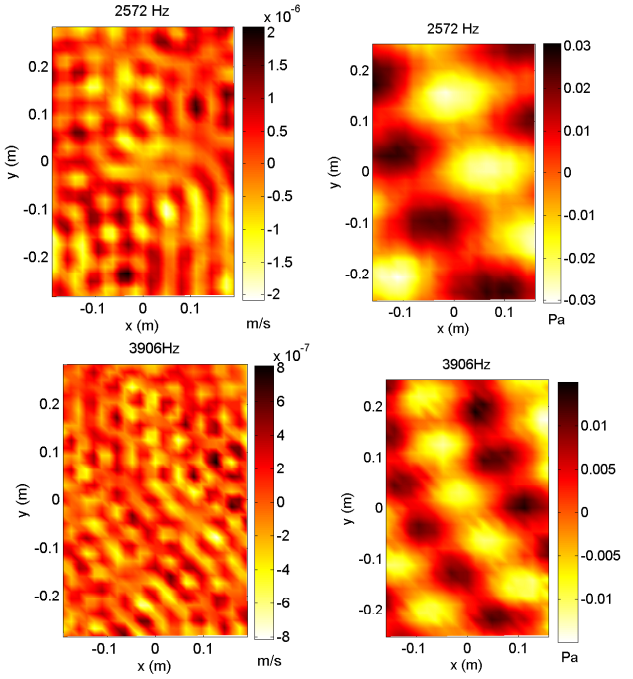

FIG. 5. (color online) Measured velocity (m/s, left) and estimated acoustic pressure (Pa, right) at 2.5kHz (top) and 4kHz (bottom). Real parts.

The beamforming is carried out using a plane wave assumption, as required in Eq. 20. This hypothesis is of course not fully satisfied, the source standing at 1.3m from the plate. This is visible in Fig. 5, on the pressure field identified at 4kHz, for which the maximum values of the pressure field are not forming a straight oblique line but a slightly curved line. However, the use of plane waves is adopted because it requires no additional hypothesis about the distance to the source.

Beamforming results are presented in Fig. 6 integrated by octave frequency bands from 1 to 4 kHz, for incidence angles varying between $-\pi/2$ and $\pi/2$ in azimuth θ and elevation φ. The maxima of the beamforming output correspond to the actual location of the source and to its ground reflection for each of the 3 octave band results, where resolution increases with frequency. It is noted that the identified image source is not perfectly symmetric to the actual source. The level is lower for the image source because of geometrical attenuation (i.e. spherical spreading), with the image source being further away from the plate. The image source received signal level is lower, simply because it is farther from the plate. Second, the ground impedance is finite, resulting in some attenuation of the reflected wave and therefore the image source (a real image source would result from the contribution of an infinite plane). Third, the source, whose axis is pointed towards the plate, is expected to become

more directional at mid and high frequencies.

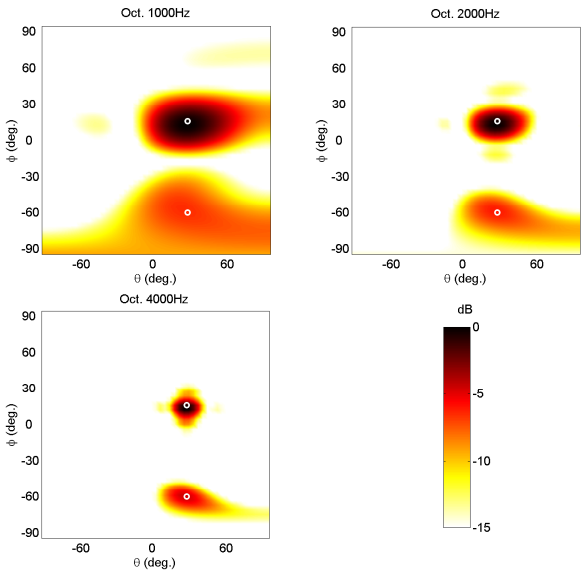

FIG. 6. (color online) Beamforming results averaged by octave bands, in dB (15dB color range), 1kHz (top left), 2kHz (top right) and 4kHz (bottom). White circles stand for the coordinates of the source and it's image generated by the reflective ground.

IV. CONCLUSION

This paper demonstrates theoretically and experimentally the feasibility of coupling two methods for the localization of acoustic sources from vibration measurements. It is shown that the wavenumber response of the corrected force analysis technique, identifying the parietal pressure, is not able to recover acoustic waves with high incident angles (high wavenumbers) when the number of points by acoustic wavelength is less than 3. Moreover, the application of CFAT requires the consideration of Shannon's sampling criterion on the plate, i.e. at least 2 points by flexural wavelength. The experimental implementation shows that the parietal pressure field is correctly identified and quantified from the vibration measurements, above a frequency limit below which some regularization would have been required. The localization of the source, as well as its image through the ground, is accurately identified on beamforming maps, demonstrating the efficiency of the proposed approach.

Acknowledgements

This work was performed within the framework of the Labex CeLyA of Université de Lyon, operated by the French National Research Agency (ANR-10-LABX-0060/ ANR-11-IDEX-0007), and supported by the Labcom P3A (ANR-13-LAB2-0011-01).

[1] C. Pezerat and J.-L Guyader, "Identification of vibration sources", Applied Acoustics **61**, 309–324 (2000).

[2] M. Djamaa, N. Ouella, C. Pezerat, and J.-L. Guyader, "Reconstruction of a distributed force applied on a thin cylindrical shell by an inverse method and spatial filtering", Journal of Sound and Vibration **301**, 560–575 (2007).

[3] C. Renzi, C. Pézerat, and J.-L. Guyader, "Vibratory source identification by using the finite element model of a subdomain of a flexural beam", Journal of Sound and Vibration **332**, 545 – 562 (2013).

[4] Q. Leclère and C. Pézerat, "Vibration source identification using corrected finite difference schemes", Journal of Sound and Vibration **331**, 1366–1377 (2012).

[5] V. M. Albers. *Underwater acoustics handbook II*. Pennsylvania State University Press, University Park, 1965, p. 356.

[6] J. Billingsley and R. Kinns, "The acoustic telescope", Journal of Sound and Vibration **48**, 485–510 (1976).

[7] B. E. Anderson, W. J. Hughes, and S. A. Hambric. On the steering of sound energy through a supercritical plate by a near-field transducer array. *The Journal of the Acoustical Society of America*, 123(5):2613–2619, 2008.

[8] A. J. Hull. Dynamic response of an insonified sonar window interacting with a tonpilz transducer array. *The Journal of the Acoustical Society of America*, 122(2):794–803, 2007.

[9] J. Moriot, L. Maxit, J.L. Guyader, O. Gastaldi, and J. Pélisse. Use of beamforming for detecting an acoustic source inside a cylindrical shell filled with a heavy fluid. *Mechanical Systems and Signal Processing*, 52-53:645 – 662, 2015.

[10] Q. Leclere and C. Pezerat, "Time domain identification of loads on plate-like structures using an array of acoustic velocity sensors", The Journal of the Acoustical Society of America **123**, 3175–3175 (2008).

[11] F. Chevillotte, Q. Leclere, N. Totaro, C. Pezerat, P. Souchotte, and G. Robert, "Identification d'un champ de pression pariétale induit par un écoulement turbulent à partir de mesures vibratoires" *(Identification of a parietal pressure field induced by a turbulent boundary layer from vibration measurements)*, in *10ème Congrès Français d'Acoustique*, (Lyon, France) (2010).

[12] D. Lecoq, C. Pézerat, J.-H. Thomas, and W. Bi, "Extraction of the acoustic component of a turbulent flow exciting a plate by inverting the vibration problem", Journal of Sound and Vibration **333**, 2505 – 2519 (2014).

[13] E. Williams, J. Maynard, and E. Skudrzyk, "Sound source reconstructions using a microphone array", Journal of the Acoustical Society of America **68**, 340–344 (1980).

[14] G. H. Koopmann, L. Song, and J. B. Fahnline, "A method for computing acoustic fields based on the principle of wave superposition", Journal of the Acoustical Society of America **86** (1989).

[15] M. Bai, "Application of bem based acoustic holography to radiation analysis of sound sources with arbitrarily shaped surfaces", Journal of the Acoustical Society of America **92** (1992).

[16] J-L. Guyader. *Vibration in continuous media*. Wiley ISTE, 2006, p. 441.

[17] Q. Leclere, "Multi-channel spectral analysis of multi-pass acquisition measurements", Mechanical System and Signal Processing **23**, 1415-1422 (2009).

[18] C. Pezerat and J.-L. Guyader, "Force analysis technique: Reconstruction of force distribution on plates", Acustica

united with Acta Acustica **86**, 322-332 (2000).

[19] Q. Leclere, F. Ablitzer, and C. Pezerat. Identification of loads of thin structures with the corrected Force Analysis technique: An alternative to spatial filtering regularization. In *Proceedings of ISMA 2014*, Leuven, Belgium, 2014.